Electronic supplementary information

Understanding sodium storage properties of ultra-small Fe_3S_4 nanoparticles – a combined XRD, PDF, XAS and electrokinetic study

Felix Hartmann,*[a] Martin Etter,[b] Giannantonio Cibin,[c] Hendrik Groß,[d] Lorenz Kienle[d] and Wolfgang Bensch*[a]

[a]Institute of Inorganic Chemistry, Christian-Albrecht University of Kiel, Max-Eyth-Str. 2, 24118 Kiel, Germany, corresponding author mail: wbensch@ac.uni-kiel.de

[b]Deutsches Elektronen-Synchrotron (DESY), Notkestr. 85, 22607 Hamburg, Germany

[c]Diamond Light Source (DLS), Harwell Science and Innovation Campus, Didcot, Oxfordshire OX11 0DE, United Kingdom

[d]Institute of Materials Science, Christian-Albrecht University of Kiel, Kaiserstr. 2, 24143 Kiel, Germany

Table S1 Structural parameters for pristine Fe_3S_4 from PDF and PXRD refinements.

Parameter	XRD	PDF
Space group	$Fd\bar{3}m$	$Fd\bar{3}m$
a / Å	9.8567(4)	9.8520(2)
Domain size	D_{vol} = 9.9(1)[a)]	D_{sph} = 10.2(1)[b)]
Fe1 (8*a*)	0.125, 0.125, 0.125	$x = y = z = 0.125$
Fe2 (16*d*)	0.5, 0.5, 0.5)	$x = y = z = 0.5$
S1 (32*e*)	0.2540(3), 0.2540(3) 0.2540(3)	0.2556(1), 0.2556(1), 0.2556(1)
DW[c)] (Fe) / Å^2	1.55(5)	1.37(1)
DW[c)] (S) / Å^2	1.77(7)	1.31(1)
R_{wp}	3.81%	13.6%
χ^2	2.58	-

[a)] Volume weighted average domain size extracted from WPPM of PXRD pattern; [b)] Spherical domain size extracted from PDF; [c)] Debye Waller factor

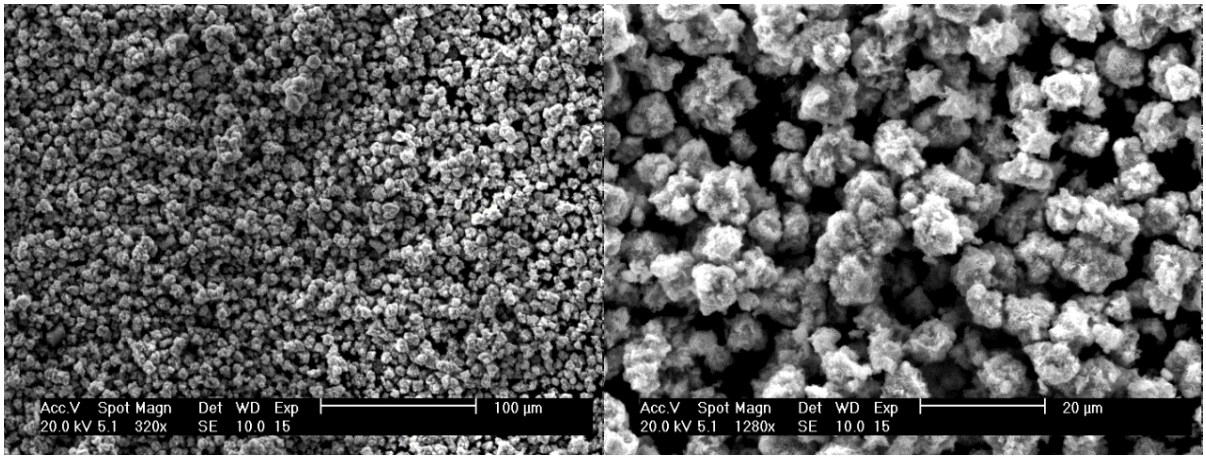

Fig. S1 SEM images of as-prepared Fe_3S_4 particles.

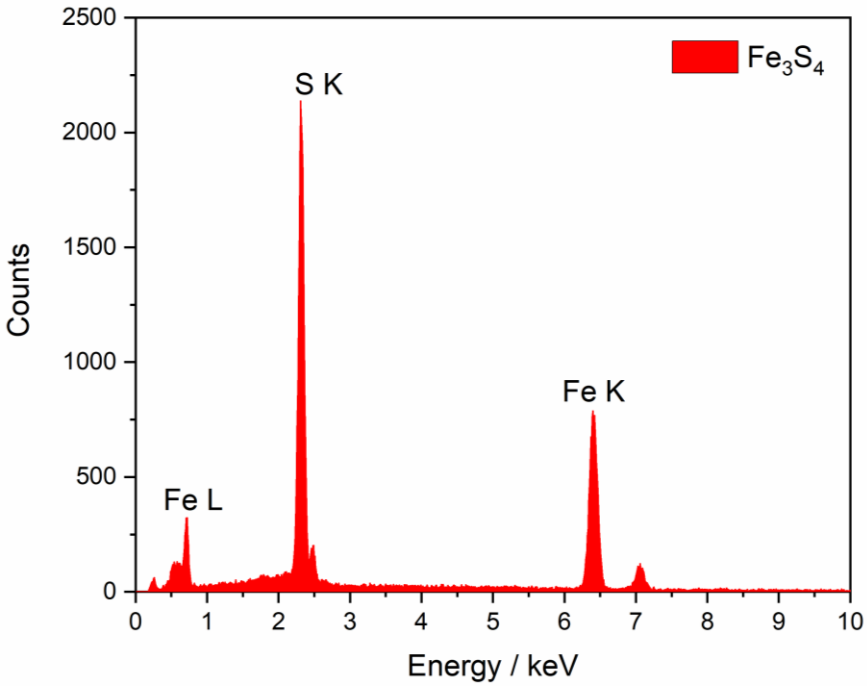

Fig. S2 EDX spectrum of as-prepared Fe_3S_4.

Table S2 Results of SEM-EDX measurements of as-prepared material.

spot	Fe / at.%	S / at.%	Stoichiometry
1	41.9	58.1	$Fe_{2.93}S_{4.07}$
2	42.1	57.9	$Fe_{2.95}S_{4.05}$
3	41.9	58.1	$Fe_{2.93}S_{4.07}$
Average	42.0 ± 0.1	58.0 ± 0.1	$Fe_{2.94(1)}S_{4.06(1)}$
Theoretical Fe_3S_4	42.9	57.1	$Fe_{3.00}S_{4.00}$

Table S3 Results of elemental anaylsis of as-prepared material. Sulphanilamide was used as reference.

measurement	N wt.%	C wt.%	H wt.%	S wt.%
1	0.39	3.00	0.43	40.47
2	0.49	3.07	0.43	40.64
Average	0.44	3.03	0.43	40.55
Theoretical Fe_3S_4	0	0	0	43.36

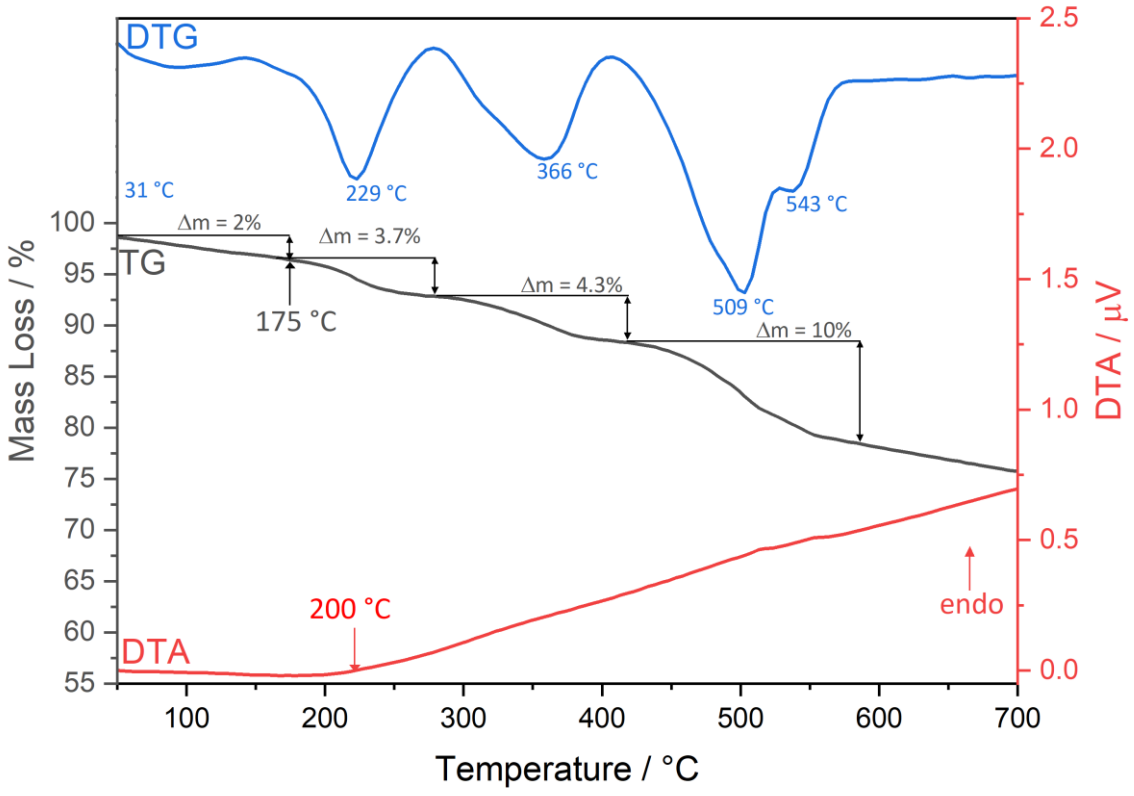

Fig. S3 Thermogravimetry (TG, black), differential thermal analysis (DTA, red) and derivative thermogravimetry (DTG, blue) of the product of solvothermal synthesis before annealing. The measurements were performed with a heating rate of 1 K min^{-1} in N_2 atmosphere.

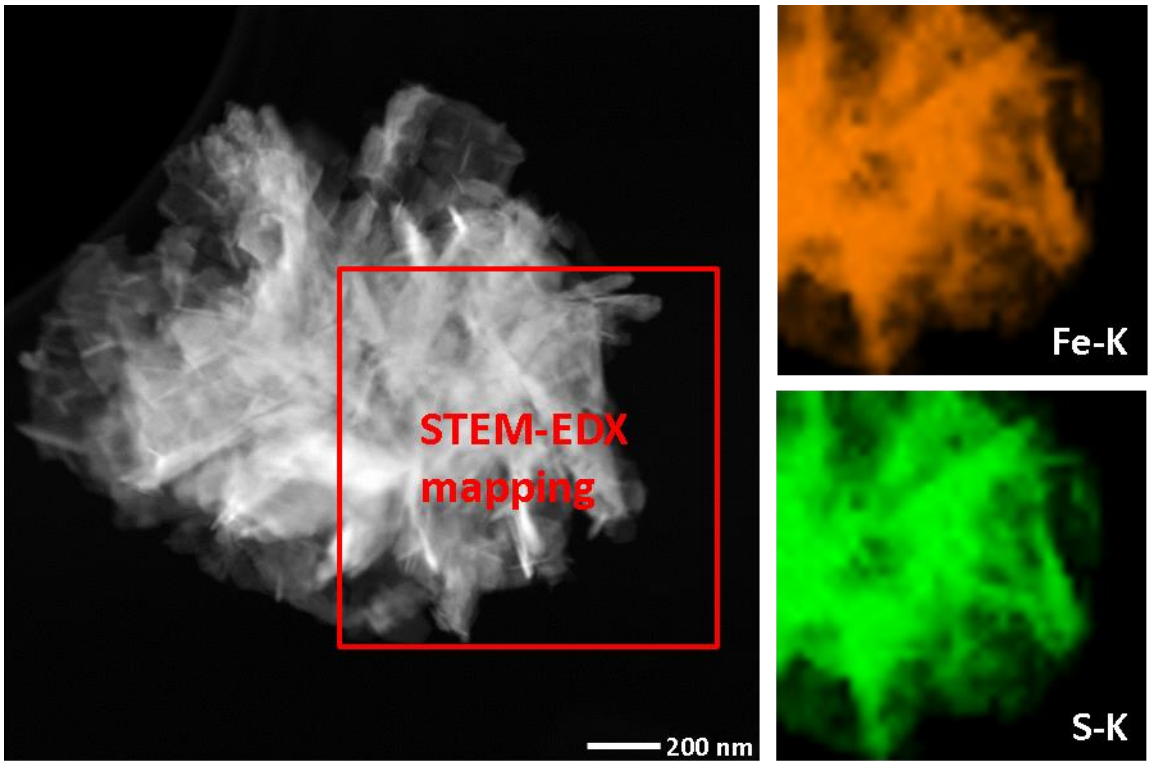

Fig. S4 STEM-EDX mapping at Fe-K and S-K edges with 40 – 50 at.% Fe and 50 – 60 at.% S content.

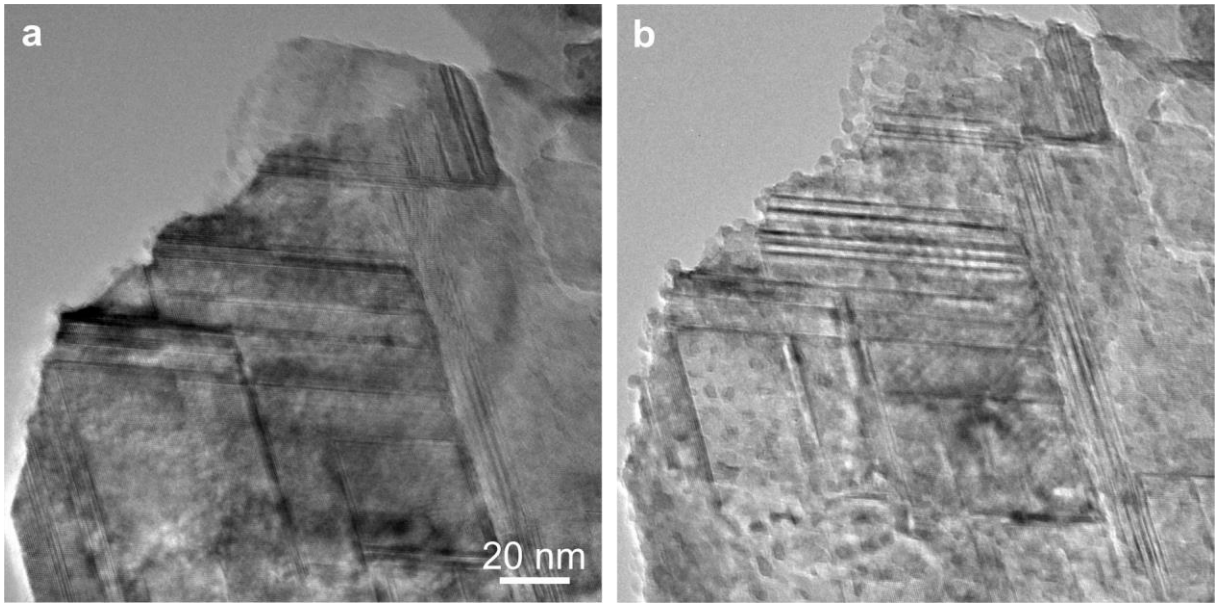

Fig. S5 HRTEM micrographs of pristine Fe_3S_4 in zone axis [$\bar{1}$10] with prominent stacking faults. a) Before and b) after prolonged exposure to electron beam irradiation.

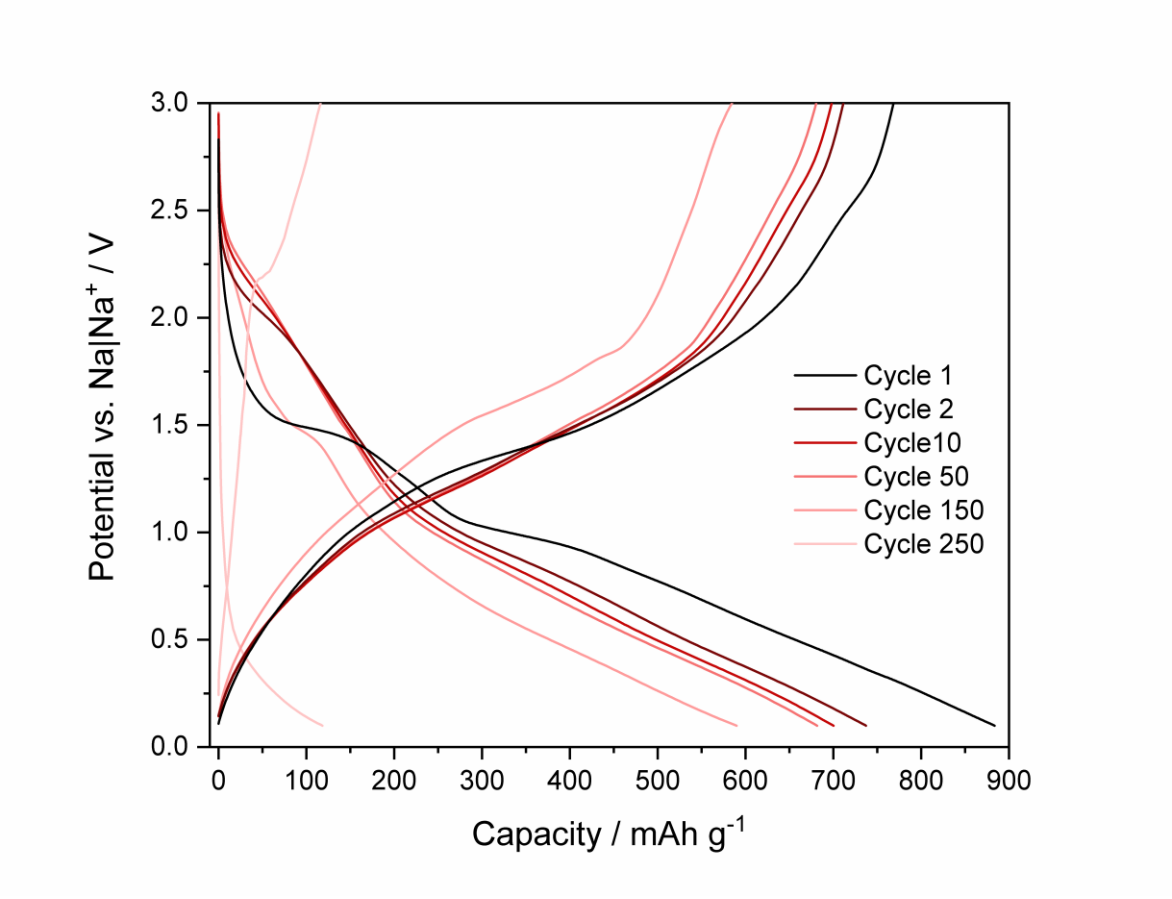

Fig. S6 GDC profiles at a current density of 0.1 A g^{-1} for the first and 0.5 A g^{-1} for subsequent cycles in the potential window 3.0 – 0.1 V.

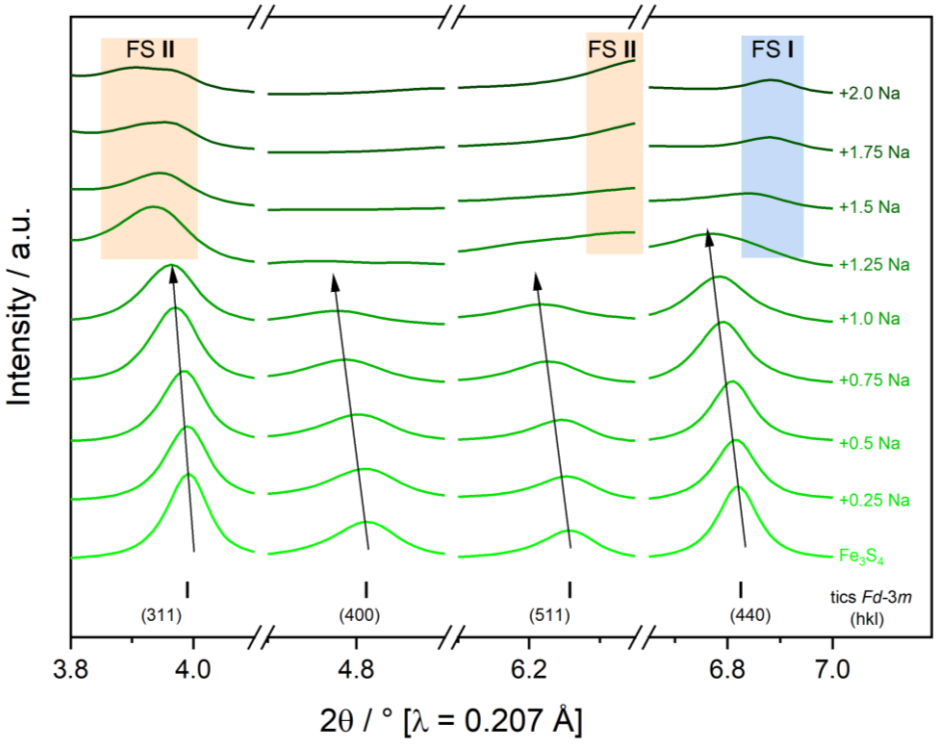

Fig. S7 Evolution of selected Fe_3S_4 XRD reflections during initial Na uptake.

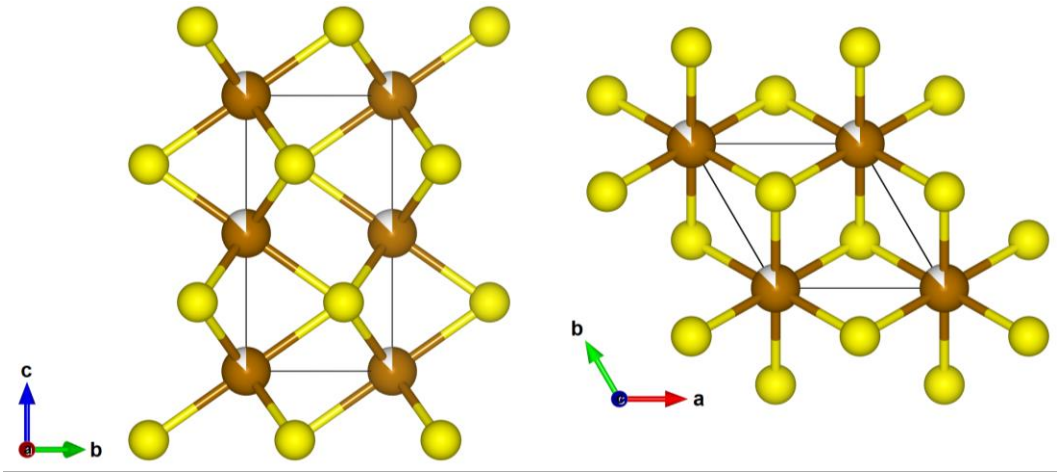

Fig. S8 Structure of $Fe_{0.88}S$ (pyrrhotite, SG: *P*6$_3$/*mmc*) along [100] (left) and [001] (right); Brown: Fe, yellow: S.

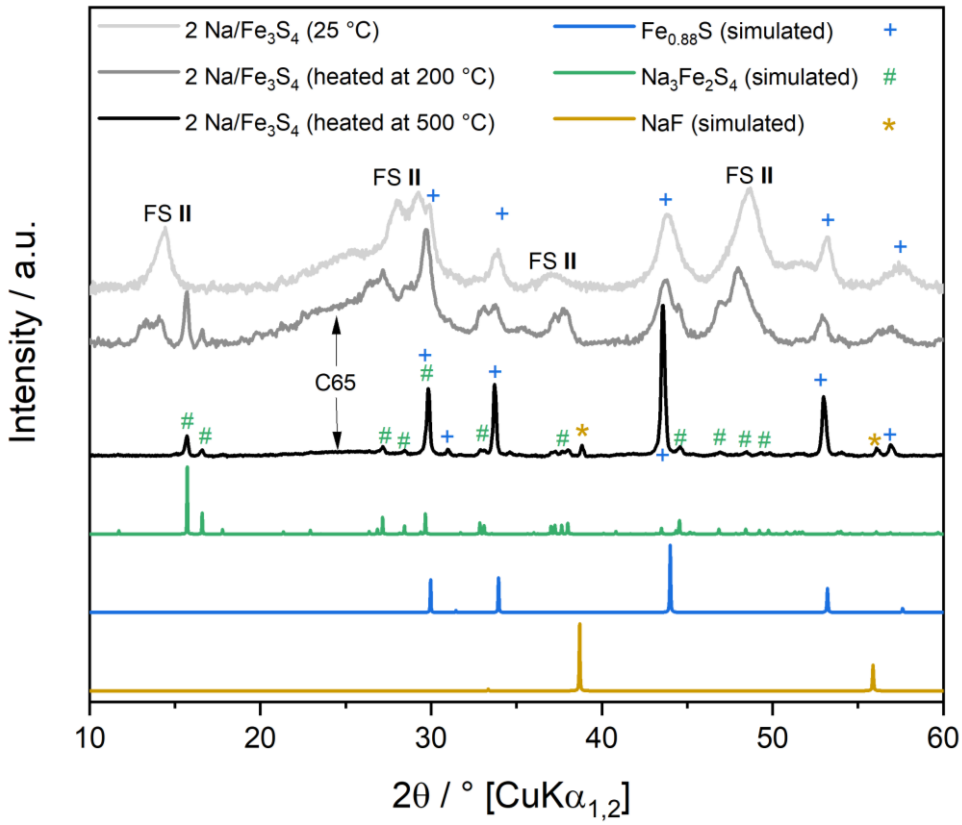

Fig. S9 Background-subtracted PXRD patterns of heat-treated (200 and 500 °C) samples containing 2 Na/Fe_3S_4 compared to simulated patterns for NaF, $Na_3Fe_2S_4$ and $Fe_{0.88}S$.

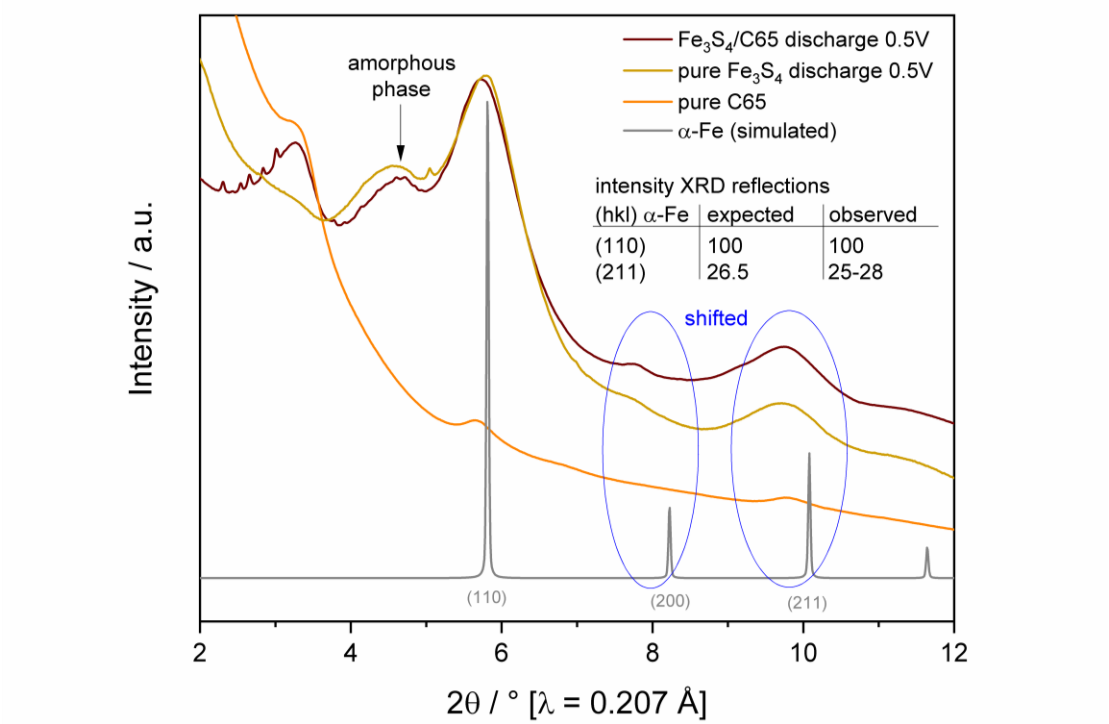

Fig. S10 Comparison of PXRD patterns collected for samples containing 70 wt.% Fe_3S_4 and 30 wt.% carbon C65 (brown) and pure Fe_3S_4 (yellow), both discharged to 0.5 V vs. Na|Na^+, pure carbon C65 (orange) and a simulated one for α-Fe (gray). The table shows expected and observed intensities for α-Fe.

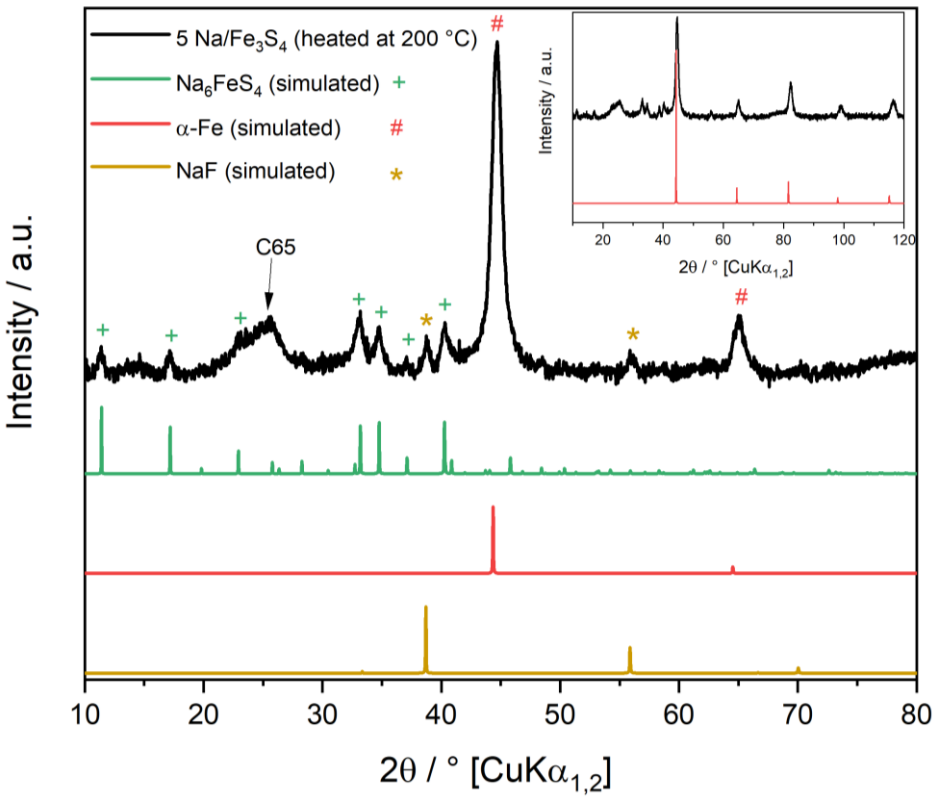

Fig. S11 Background-subtracted PXRD patterns of a heat-treated (200 °C) sample containing 5 Na/Fe_3S_4 compared to simulated patterns for NaF, Na_6FeS_4 and α-Fe. The inset shows the same PXRD pattern to 120° 2θ with observed reflections clearly matching those of α-Fe.

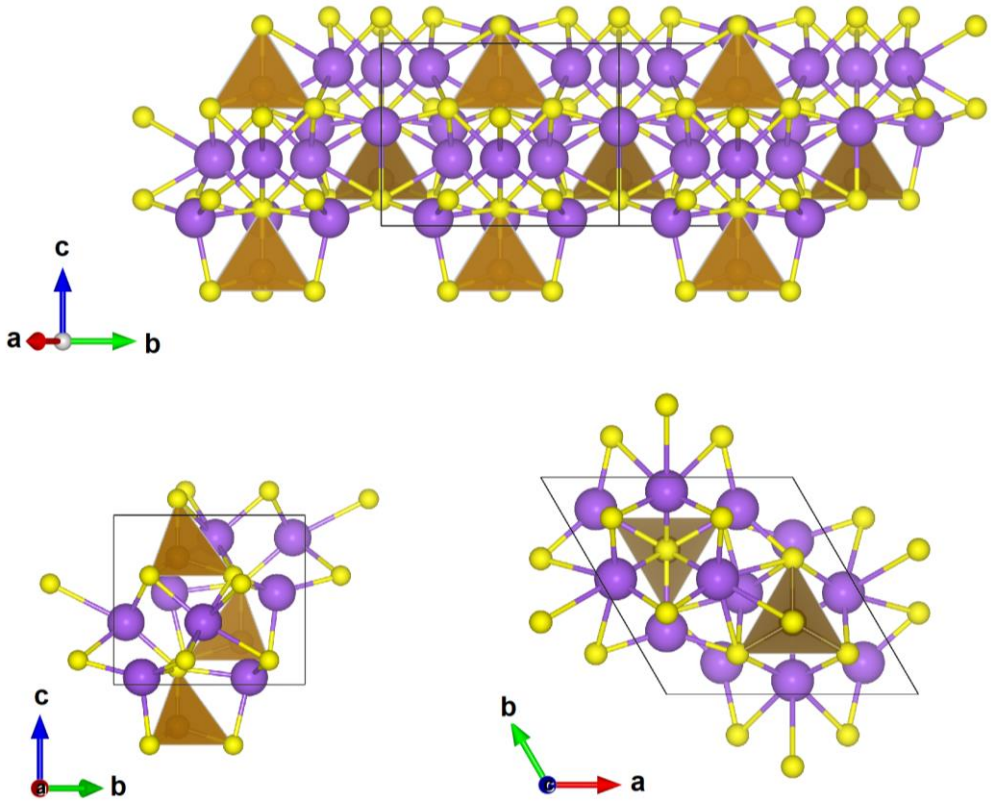

Fig. S12 Structure of Na_6FeS_4 (SG: *P*6$_3$*mc*): Brown tetrahedra represent single FeS_4 units, NaS_4 tetrahedra and NaS_6 octahedra are not shown;[1] Brown: Fe, purple: Na, yellow: S.

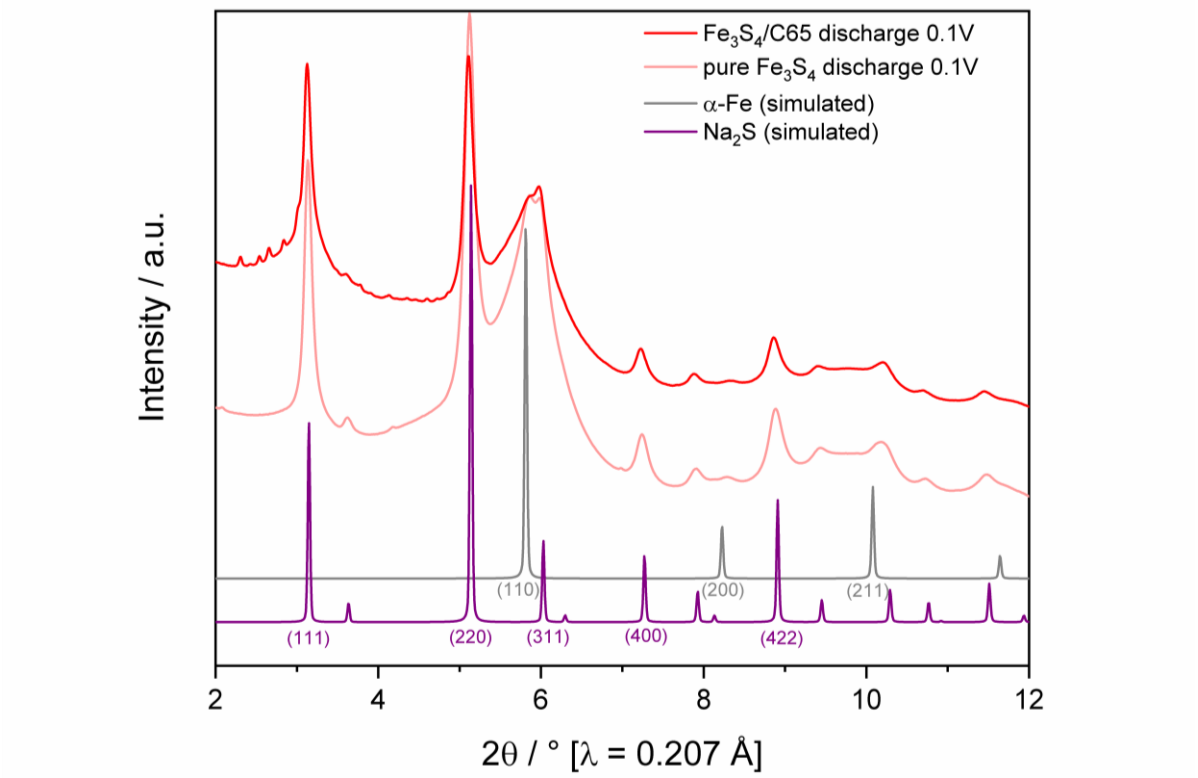

Fig. S13 Comparison of PXRD patterns collected for samples containing 70 wt.% Fe_3S_4 and 30 wt.% carbon C65 (red) and pure Fe_3S_4 (light red), both discharged to 0.1 V vs. Na|Na^+, and simulated ones for α-Fe (gray) and Na_2S (purple).

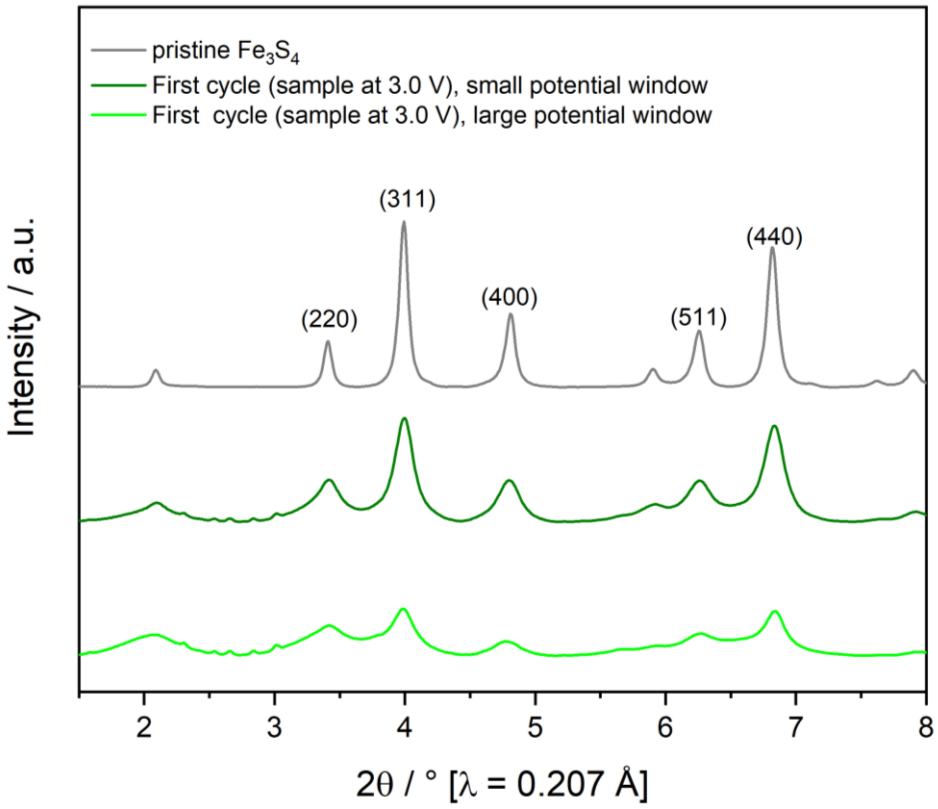

Fig. S14 PXRD patterns of pristine Fe_3S_4 (gray), after the first cycle in 3.0 – 0.5 V (dark green) and in 3.0 – 0.1 V (light green).

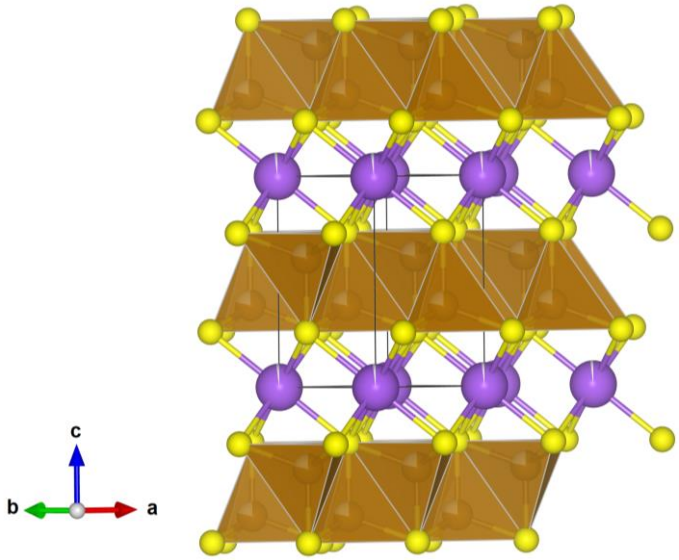

Fig. S15 Structure of $NaFe_{1.6}S_2$ (SG: $P\bar{3}m1$): Brown polyeder represent edge-sharing FeS_4 tetrahedra, which form $[Fe_{1.6}S_2]^-$ layers in the *a*/*b* plane hosting Na^+ ions (purple) on octahedral interlayer sites;[2] Brown: Fe, purple: Na, yellow: S.

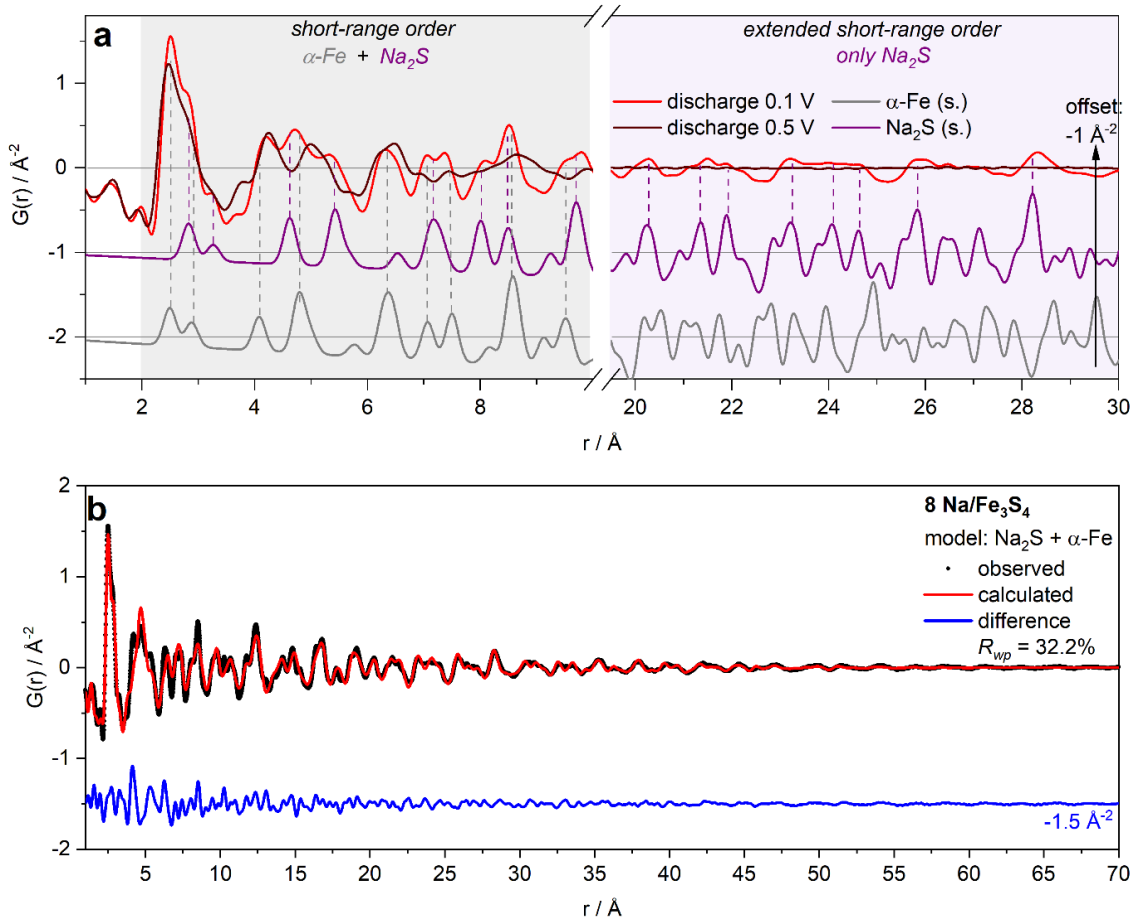

Fig. S16 a) Comparison of PDFs calculated for samples discharged to 0.5 and 0.1 V, respectively, to simulated PDFs for α-Fe and Na_2S with spherical shapes (D_{sph} = 20 nm); b) Modelling of the PDF of the sample discharged to 0.1 V (8 Na/Fe_3S_4) to α-Fe and Na_2S.

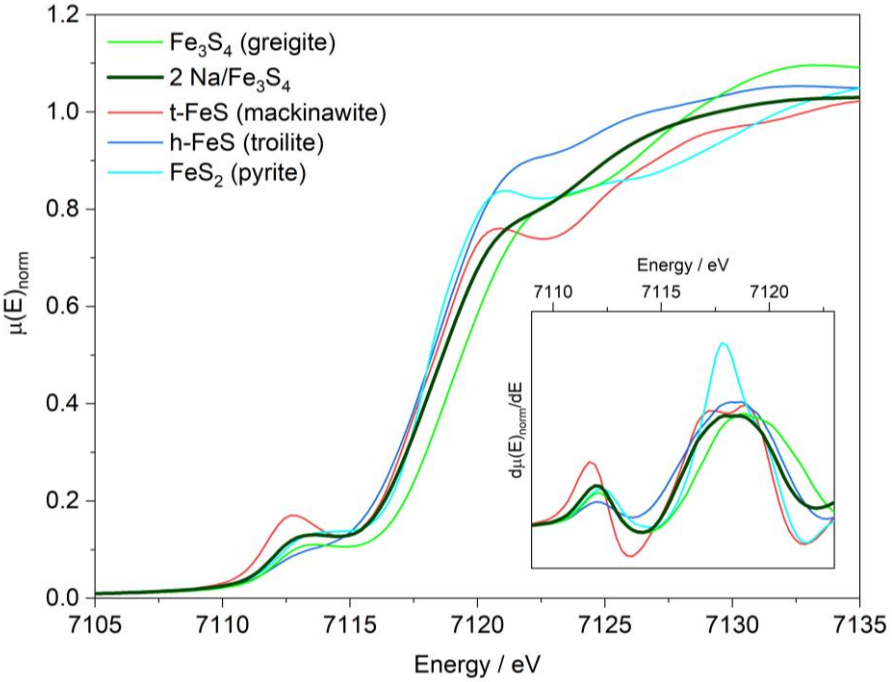

Fig. S17 XANES spectra of a sample containing 2 Na/Fe_3S_4 compared to reference spectra of t-FeS (mackinawite), h-FeS (troilite), FeS_2 (pyrite) and Fe_3S_4 (greigite). The inset shows corresponding deviations $d\mu(E)_{norm}/dE$.

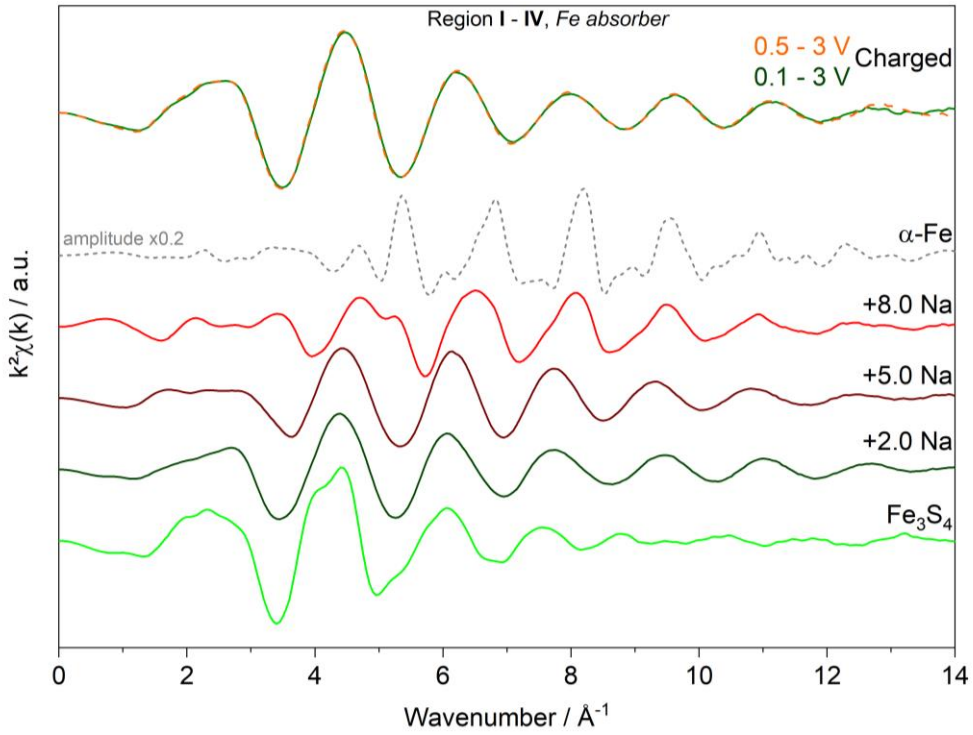

Fig. S18 Evolution of *k* space EXAFS spectra (Fe absorber) during Na uptake/release in Fe_3S_4.

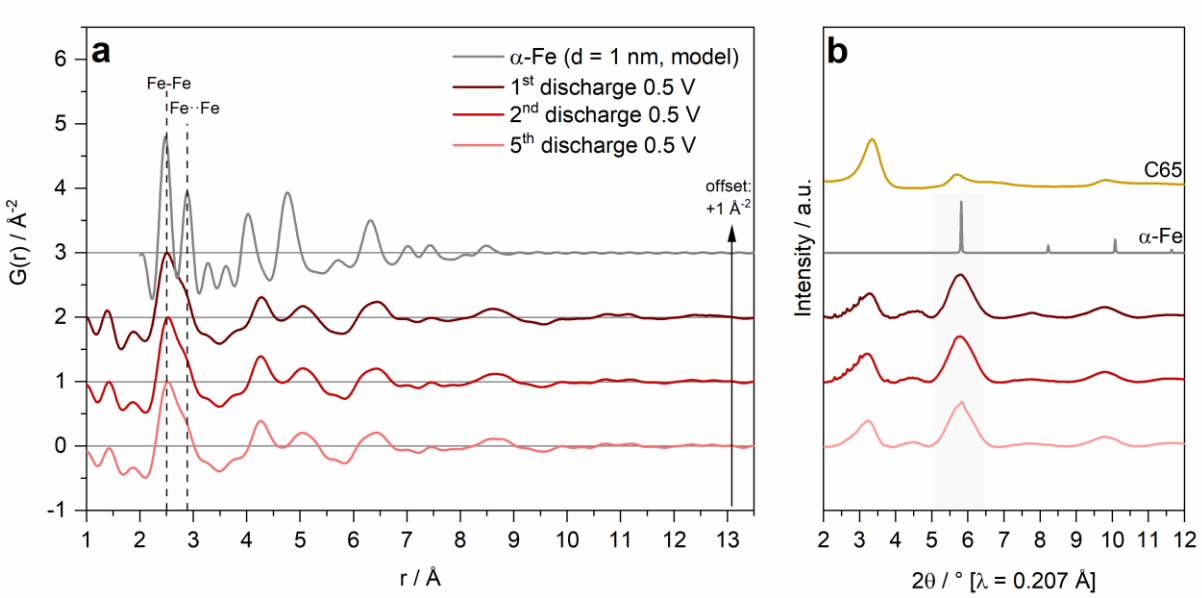

Fig. S19 a) PDFs calculated for discharged samples (0.5 V) in the first, second and fifth cycle applying the small potential window and b) corresponding PXRD patterns compared to one for carbon C65 and a simulated one for α-Fe.

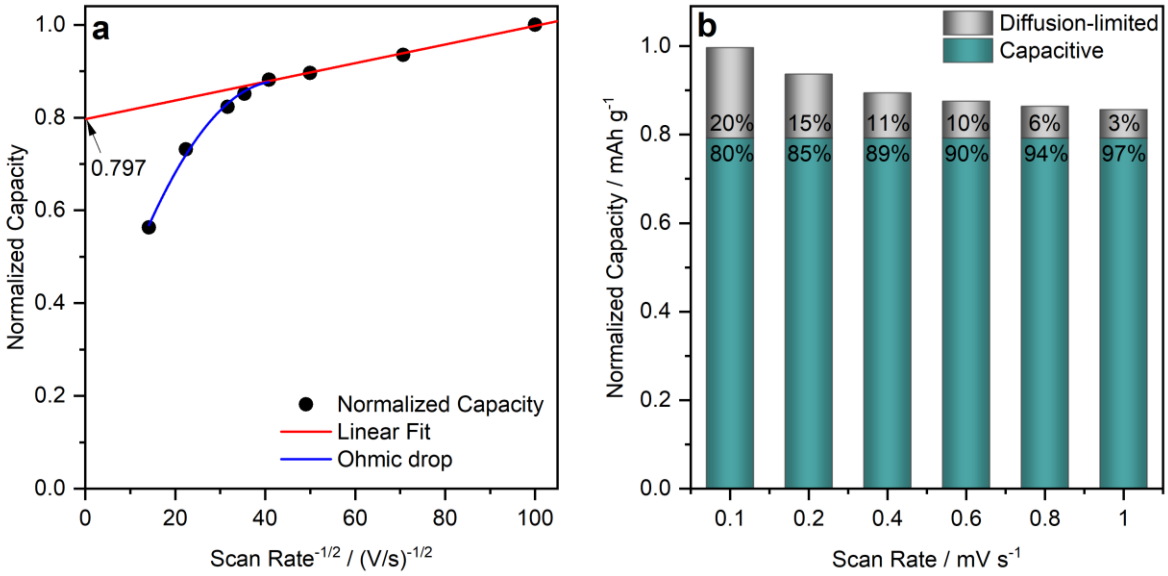

Fig. S20 a) Infinite scan rate extrapolation (Trasatti method)[3–5] for small scan rates where the Ohmic drop is neglectable and b) quantities extracted from this method.

References in Supplementary Information

1 W. Bronger, H. Balk-Hardtdegen and U. Ruschewitz, *Z. Anorg. Allg. Chem.*, 1992, **616**, 14–18.

2 X. Lai, X. Chen, S. Jin, G. Wang, T. Zhou, T. Ying, H. Zhang, S. Shen and W. Wang, *Inorg. Chem.*, 2013, **52**, 12860–12862.

3 S. Ardizzone, G. Fregonara and S. Trasatti, *Electrochim. Acta*, 1990, **35**, 263–267.

4 G. Zou, Q. Zhang, C. Fernandez, G. Huang, J. Huang and Q. Peng, *ACS Nano*, 2017, **11**, 12219–12229.

5 V. Augustyn, J. Come, M. A. Lowe, J. W. Kim, P.-L. Taberna, S. H. Tolbert, H. D. Abruña, P. Simon and B. Dunn, *Nat. Mater.*, 2013, **12**, 518–522.